ELSEVIER

Physica D 101 (1997) 249–269

PHYSICA D

Period-doubling for two-dimensional non-invertible maps: Renormalization group analysis and quantitative universality

S.P. Kuznetsov *, I.R. Sataev

Institute of Radio-Engineering and Electronics, Russian Academy of Sciences, Zelenaya, 38, Saratov 410019, Russian Federation

Received 21 September 1995; revised 16 July 1996; accepted 15 September 1996
Communicated by F.H. Busse

Abstract

Two types of universal behavior associated with period-doubling in two-dimensional non-invertible maps are investigated. The first, called C-type, may occur as a generic two-parameter phenomenon when the map possesses a fold singularity. The second kind of universal behavior, called FQ-type, is associated with the singularity arising from projecting Whitney's umbrella. Typically, this kind of period-doubling scaling behavior appears as a phenomenon of codimension three, i.e. at some critical point in the three-dimensional parameter space. Numerical results are presented to illustrate the self-similarity of the parameter space topography near the critical points C and FQ. The possibility of observing these new types of critical behavior in physical systems is discussed.

Keywords: Period-doubling; Non-invertible map; Whitney's umbrella

1. Introduction

The well-known Feigenbaum universality occurs in many nonlinear dissipative systems including one-dimensional non-invertible maps. It appears as a typical phenomenon in a one-parameter analysis of the transition to chaos via a period-doubling cascade. This kind of critical behavior at the border of chaos is associated with a certain saddle fixed point of the functional renormalization-group (RG) equation of Feigenbaum–Cvitanovic [1–3].

$$g(x) = \alpha g(g(x/\alpha)). \tag{1}$$

This fixed point solution is represented by a universal function $g(x) = 1 - 1.5276x^2 + 0.1048x^4 + \cdots$, which has a quadratic extremum at the origin. The scaling factor α is a universal number equal to $-2.5029\ldots$.

For one-dimensional maps with several control parameters some particular paths in the parameter space may exist giving rise to behavior associated with other fixed points of the functional equation (1). The corresponding

* Corresponding author. E-mail: kuz@spkuz.saratov.su.

PII S0167-2789(96)00237-0

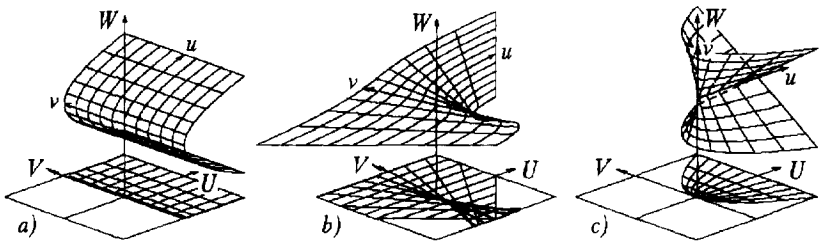

Fig. 1. Geometrical representation of the singularities of the two-dimensional maps: (a) fold; (b) cusp; (c) projection of Whitney's umbrella.

functions $g(x)$ may have extrema of the order $z = 4, 6, 8, \ldots$, and the scaling factor α depends on z [4–6]. Thus, a multi-parameter analysis of the transition to chaos may lead to various universality classes and critical behavior types.

For one-dimensional maps a certain universality class is associated with a definite order of the extremum, i.e. with the nature of the point of zero derivative. For two-dimensional maps $(x, y) \to (g(x, y), f(x, y))$, a similar role must be played by singular points or lines in (x, y) plane at which the Jacobi determinant

$$J = \begin{vmatrix} \partial g/\partial x & \partial g/\partial y \\ \partial f/\partial x & \partial f/\partial y \end{vmatrix}$$

is equal to zero (see also [7]).

Two-dimensional maps may be represented geometrically. Let us consider some curved surface S in three-dimensional space (U, V, W), and define a coordinate system (u, v) on this surface. It means that we have some mapping of the two-dimensional space into the three-dimensional space: $(u, v) \to (U, V, W)$. Next, let us project the surface S, say, onto the plane (U, V) along the W-axis. As a result, we obtain a two-dimensional map $(u, v) \to (U, V)$. There are two sources of singularities of this map. First, a singularity appears when the projective direction coincides at some point with a direction tangential to the surface S. Alternatively, the surface S may have some singularity itself, inducing a singularity also in the two-dimensional map.

Classification of singularities for differentiable maps is developed in mathematical texts [8–10]. It is proved that a generic two-dimensional map may possess only two types of singularities: *folds* and *cusps* (Figs. 1(a) and (b)). The only generic singularity for a map from two-dimensional space into three-dimensional space is represented geometrically by a remarkable surface – *Whitney's umbrella* (Fig. 1(c)).

Suppose we have a two-dimensional map exhibiting a period-doubling cascade with specific properties of universality and scaling associated with a certain type of singularity of the map. The same singularity must be inherent in the solution of the two-dimensional generalized Feigenbaum–Cvitanovic equation. So, the problem is: Can we find solutions of this RG equation with singularities of definite types?

In this paper we consider two types of criticality associated with period-doubling in two-dimensional non-invertible maps. These types of behavior were discussed briefly in our previous publication [11] and are called C-type and FQ-type, respectively. Here we present simpler model maps and discuss in more detail the peculiarities of the critical dynamics, the parameter space topography near the critical points, and scaling properties in phase space and parameter space.

The criticality of C-type occurs when the map possesses the simplest fold singularity, and may appear as a typical phenomenon in a two-parameter analysis of the period-doubling transition to chaos. A remarkable property of this critical point is the presence of an infinite self-similar set of attractors – stable cycles of period 4^k or 2×4^k, $k = 0, 1, 2, \ldots$. We call this set *critical quasi-attractor*.

Another kind of critical behavior, FQ, occurs when the map has a singularity which arises from the projection of Whitney's umbrella. In general, the codimension of the FQ-type criticality is three. At the critical point FQ the map has a complete set of unstable period-2^k cycles. The attractor is a fractal Cantor-like set embedded in the two-dimensional phase space.

For the cusp singularity we have not found the quantitative universality associated with period-doubling. We think that there is no one-to-one correspondence: particular interesting types of critical behavior do not arise from all possible singularities of differentiable two-dimensional maps.

2. RG transformation and two-dimensional generalization of Feigenbaum–Cvitanovic equation

Suppose we have a two-dimensional map

$$G_0: \qquad X_{n+1} = g_0(X_n, Y_n), \quad Y_{n+1} = f_0(X_n, Y_n). \tag{2}$$

Let us apply it twice to obtain a map describing two-time-step evolution. Then, we introduce a linear variable transformation S to make the new map $G_1 = S^{-1}G_0G_0S$ as similar to G_0 as possible. We suppose that the coordinate system (X, Y) is chosen in such a way that the above variable change has a diagonal form, i.e. $S: X \to X/\alpha, Y \to Y/\beta$. We can apply the same procedure recurrently to the map G_1 and obtain a map $G_2 = S^{-1}G_1G_1S$, and so on. Multiple repetition of the procedure generates a sequence of maps G_k:

$$G_{k+1} = S_k^{-1}G_kG_kS_k. \tag{3}$$

A map G_k is a renormalized evolution operator which expresses the result of 2^k iterations of the original map. Explicitly, in terms of functions g and f, Eq. (3) implies

$$\begin{aligned} g_{k+1}(X, Y) &= \alpha_k g_k(g_k(X/\alpha_k, Y/\beta_k), f_k(X/\alpha_k, Y/\beta_k)), \\ f_{k+1}(X, Y) &= \beta_k f_k(g_k(X/\alpha_k, Y/\beta_k), f_k(X/\alpha_k, Y/\beta_k)). \end{aligned} \tag{4}$$

Usually, it is convenient to impose the normalization condition:

$$g(0, 0) = 1, \quad f(0, 0) = 1. \tag{5}$$

In accordance with (4) it means that

$$\alpha_k = 1/g_k(1, 1), \qquad \beta_k = 1/f_k(1, 1). \tag{6}$$

In the framework of the RG analysis, each type of universal critical behavior is associated with a saddle fixed point or a saddle cycle of the functional mapping defined by (4)–(6). (We will not consider non-periodic saddle orbits analogous to those discussed in [12] for one-dimensional maps.)

Using orthogonal polynomial expansions for the unknown functions g and f one can take advantage of standard numerical techniques to find solutions of the functional equation (4). (Note that a crucial condition for obtaining a solution is the necessity to have good initial approximation.) One known fixed point of the RG equations is related to the Hamiltonian type of criticality for area-preserving maps [13,14]. Several new solutions (in particular, for such two-dimensional maps that may be partitioned into subsystems with uni-directional coupling) were found and studied in our papers [11,15,16].

When the solution is found (either a fixed point or a cycle) the eigenvalue spectrum of the linearized RG transformation must be studied. The number of relevant unstable directions (i.e. the number of eigenvalues that are greater than unity in modulus and are not related to infinitesimal variable changes) define *the codimension*. This is the

number of parameters for the family of systems in which the given type of critical behavior occurs as a generic phenomenon. In other words, to consider unfolding of the critical situation, we must introduce this number of control parameters. The relevant eigenvalues define scaling factors along appropriate directions in the parameter space.

3. Critical behavior for the maps with fold singularity

3.1. Model map and location of the critical points

The standard form of a two-dimensional map in the vicinity of the fold singularity is as follows:

$$(u, v) \to (u^2, v). \tag{7}$$

Composition of (7) with a general affine transformation gives the map $(u, v) \to (A + Bu^2 + Cv, D + Eu^2 + Fv)$. Using the change of variables

$$x = -Bu, \quad y = [D/(1 - F) - v]B^2/F, \quad a = B[CD/(F - 1) - A], \quad b = EC/B, \quad d = F, \tag{8}$$

we obtain a map with three parameters

$$x_{n+1} = a - x_n^2 + by_n, \qquad y_{n+1} = -x_n^2 + dy_n. \tag{9}$$

Fig. 2 shows the topography of the dynamical regimes for the map (9) in the parameter plane (a, d) for $b = -0.6663$ and 0.6544. (The reason for choosing these values of b is given below.) The usual Feigenbaum period-doubling cascade is observed in the left part of Fig. 2(a) and in the bottom part of Fig. 2(b). The border of chaos is Feigenbaum's critical line (a locus of accumulation of the period-doubling bifurcation curves). For larger d we see changes in the dynamics; in particular, saddle–node bifurcations appear.

Let us choose negative b for definiteness. For some small d we may find the value of a for the ith period-doubling bifurcation of the map (9). Then, the period-2^i cycle has one multiplier $\mu_1 = -1$ while the second multiplier μ_2 is in the vicinity of zero. Now let us increse d and continuously tune a to keep $\mu_1 = -1$. Moving in such a way along the bifurcation curve, we arrive at a point (a_i, d_i) where μ_2 reaches 1. We call this codimension-two bifurcation point *terminal*. The calculations show that each line of the period-doubling has its own terminal point (Table 1). We conjecture that the terminal points form an infinite cascade. Estimating the limit of the sequence of terminal points, we obtain the sought-for critical point of C type (a_c, d_c). Incidentally, we estimate also the limit for a sequence of the initial points of periodic orbits for $i \to \infty$: $x_c = \lim x_0^{(i)} = 0$, $y_c = \lim y_0^{(i)}$. In general, the observed convergence is very slow, but it may be substantially improved by choosing a proper value of $b = -0.6663$. In this case we obtain

$$a_c = 0.249902800, \quad d_c = 0.452902880, \quad y_c = -1.316447534. \tag{10}$$

Also for $b > 0$ the critical point of C-type may be found from the same procedure. The best convergence occurs at $b = 0.6544$ (see Table 1), and we obtain

$$a_c = 0.566620683, \quad d_c = 1.597132592, \quad y_c = 1.709352174. \tag{11}$$

3.2. Solution of the RG equation: Period-2 saddle cycle and its perturbations

Now we have to answer the question: What is the nature of the solution for the RG equation corresponding to the critical points? To this end, let us take the map (9) at the C-point and consider the sequence of maps G_k generated

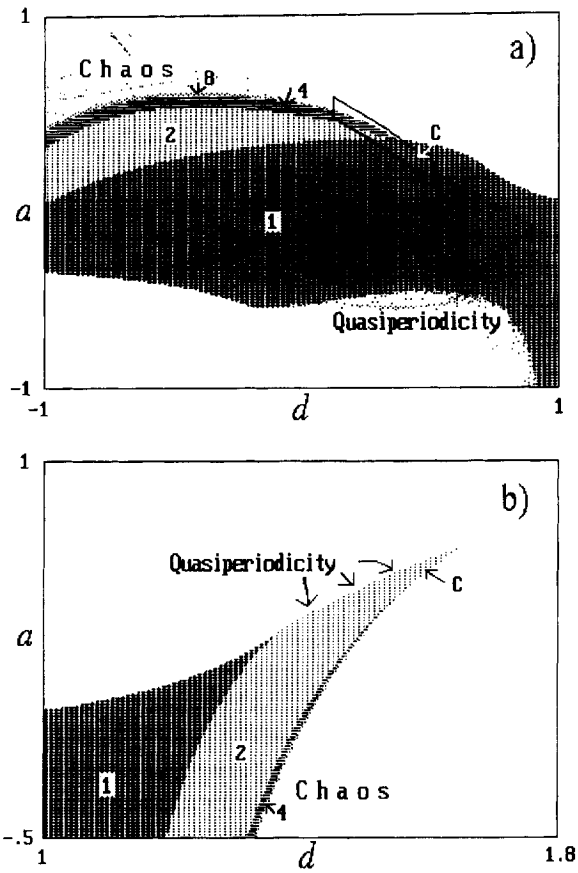

Fig. 2. Topography of the parameter plane (a, d) for the map (9), $b = -0.6663$ (a), and $b = 0.6544$ (b). The stability domains for cycles of different periods are shown with different shading; periods are indicated by numbers. A curvilinear quadrangle corresponds to the region shown in the top picture of Fig. 6.

Table 1
Terminal points at the period-doubling bifurcation curves for the map (9)

Period	$b = -0.6663$		$b = 0.6544$	
	a	d	a	d
1	0.18022115	0.72088459	0.34484228	1.3793691
2	0.33342500	0.33370000	0.66360000	1.6544000
4	0.20496548	0.48791968	0.45134332	1.5473421
8	0.28649167	0.42178243	0.59396560	1.6099219
16	0.23978391	0.46079558	0.53889271	1.5847814
32	0.25943497	0.44525313	0.57325234	1.6001622
64	0.24753663	0.45476595	0.56002970	1.5941533
128	0.25221811	0.45106677	0.56820725	1.5978543
256	0.24934120	0.45334626	0.56505051	1.5964201
∞	0.24990280	0.45290288	0.56662068	1.5971326

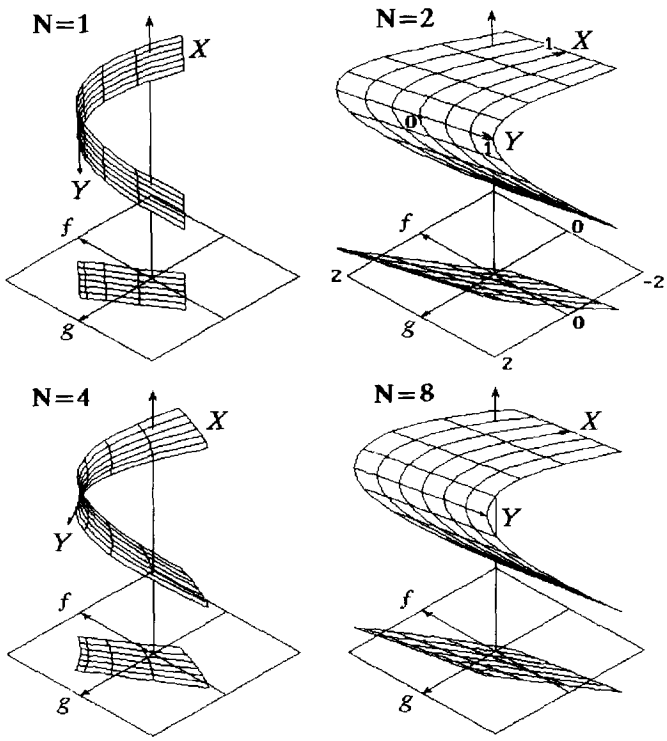

Fig. 3. Geometrical representation of the renormalized two-dimensional maps G_k obtained from N-fold iterations of the map (9) and the C-type critical point (10). Observe that the G_k sequence approaches a cycle of period 2.

by iterations of the RG transformation (4). To obtain good asymptotic behavior of the sequence G_k, it is necessary to shift the origin to the point $(0, y_c)$ and assume $X = x$ and $Y = y - y_c$. So, we define

$$g_0(X_n, Y_n) = a_c - X_n^2 + b(Y_n + y_c), \qquad f_0(X_n, Y_n) = -X_n^2 - y_c + d_c(Y_n + y_c), \tag{12}$$

and take the map

$$G_0 : \qquad X_{n+1} = g_0(X_n, Y_n), \quad Y_{n+1} = f_0(X_n, Y_n), \tag{13}$$

as initial condition for the iteration procedure (4).

Note that $G_k : (X, Y) \to \{g_k(X, Y), f_k(X, Y)\}$ is simply the normalized shifted map describing the dynamics of the original map over 2^k steps. So, the functions g_k and f_k may be computed as follows. First, we iterate the map (13) $N = 2^k$ times starting from $X_0 = 0$, $Y_0 = 0$, and denote the result as $(\bar{X}_N, \bar{Y}_N)$. Next, given the initial values $X_0 = X \cdot \bar{X}_N$, $Y_0 = Y \cdot \bar{Y}_N$, we again iterate (13) N times and obtain X_N and Y_N. Finally

$$g_k(X, Y) = X_N/\bar{X}_N, \quad f_k(X, Y) = Y_N/\bar{Y}_N, \qquad N = 2^k. \tag{14}$$

Fig. 3 shows the plots for the maps G_k obtained at the point (10). Apparently, with increasing k the sequence of maps G_k behaves as *a period-2 cycle* of the RG equation. (Such cyclic behavior accounts for the symbol "C" chosen to denote this type of criticality.) At the point (11) the same "RG cycle" is realized, but it oscillates with opposite phase.

Table 2
Polynomial approximations for the functions g_1, f_1, g_2, f_2, corresponding to period-2 saddle cycle of the RG equation (4)

	1	x^2	x^4	x^6	x^8	x^{10}	x^{12}	x^{14}	x^{16}
$g_1(x, y)$									
1	1.00000	−1.27700	0.08729	0.00628	−0.00077	0.00002			
Y	−0.49955	0.13906	0.00422	−0.00178	0.00012				
Y^2	0.04634	−0.00148	−0.00142	0.00018					
Y^3	−0.00108	−0.00045	0.00012	−0.00001					
Y^4	−0.00004	0.00004	−0.00001						
$f_1(x, y)$									
1	1.00000	−2.32102	0.39699	0.00170	−0.00489	0.00043			
Y	0.22671	0.50507	−0.03003	−0.00829	0.00144	−0.00003	−0.00001		
Y^2	0.14401	−0.03241	−0.00414	0.00173	−0.00012	−0.00001			
Y^3	−0.00869	−0.00035	0.00096	−0.00014					
Y^4	0.00014	0.00024	−0.00008						
Y^5	0.00002	−0.00002							
$g_2(x, y)$									
1	1.00000	−1.52925	0.01940	0.04473	−0.00383	−0.00013	0.00004		
Y	0.23143	−0.05923	−0.02455	0.00454	−0.00003	−0.00006			
Y^2	0.00999	0.00381	−0.00179	0.00010	0.00003				
Y^3	−0.00013	0.00029	−0.00004	−0.00001					
Y^4	−0.00002	0.00001							
$f_2(x, y)$									
1	1.00000	−1.65976	−1.44352	0.4013	0.00759	−0.00668	0.00010	0.00014	−0.00002
Y	1.34915	0.22124	−0.27816	0.01273	0.00723	−0.00061	−0.00017	0.00004	
Y^2	0.00144	0.05558	−0.01033	−0.00266	0.00056	0.00007	−0.00003		
Y^3	−0.00324	0.00229	0.00038	−0.00022	−0.00001	0.00001			
Y^4	−0.00016	−0.00001	0.00004						

The relevant solution of Eq. (4) consists of two pairs of functions (g_1, f_1) and (g_2, f_2) satisfying a set of equations:

$$
\begin{aligned}
g_2(X, Y) &= \alpha_1 g_1(g_1(X/\alpha_1, Y/\beta_1), f_1(X/\alpha_1, Y/\beta_1)),\\
f_2(X, Y) &= \beta_1 f_1(g_1(X/\alpha_1, Y/\beta_1), f_1(X_1\alpha_1, Y/\beta_1)),\\
g_1(X, Y) &= \alpha_2 g_2(g_2(X/\alpha_2, Y/\beta_2), f_2(X/\alpha_2, Y/\beta_2)),\\
f_1(X, Y) &= \beta_2 f_2(g_2(X/\alpha_2, Y/\beta_2), f_2(X/\alpha_2, Y/\beta_2)),
\end{aligned}
\tag{15}
$$

where

$$
\alpha_{1,2} = 1/g_{1,2}(1, 1), \qquad \beta_{1,2} = 1/f_{1,2}(1, 1). \tag{16}
$$

In other words, each pair of the functions, (g_1, f_1) and (g_2, f_2), is the fixed point for the *quadrupling* RG transformation (twice the iteration of transformation (4)).

To find the solution numerically with high precision we approximate $g_{1,2}(X, Y)$ and $f_{1,2}(X, Y)$ by truncated polynomial expansions, reduce (15) to a finite set of nonlinear algebraic equations for the coefficients, and solve them by the Newton–Raphson technique. Any map G_k computed from (12)–(14) may be taken as an initial guess. In Table 2 we present the polynomial expansions for both pairs of functions forming the RG cycle.

We define the scaling factors for the dynamical variables X and Y over the period of the RG cycle as

$$
\alpha_* = (\alpha_1\alpha_2) = 6.565350 \quad \text{and} \quad \beta_* = (\beta_1\beta_2) = 22.120227. \tag{17}
$$

Obviously, these are the scaling factors for the quadrupling RG transformation.

By linearizing (15) one can derive the eigenproblem associated with evolution of the perturbation over one period of the RG cycle. Here we do not write out these cumbersome equations, but we have solved the eigenproblem numerically. The three largest eigenvalues (that are not associated with infinitesimal variable changes) are:

$$\delta_1 = 92.43126348, \quad \delta_2 = 4.19244418, \quad \delta_3 \approx 0.93, \quad \ldots \tag{18}$$

We see that the RG cycle is of a saddle type.

It is clear that only δ_1 and δ_2 give rise to growing perturbations of the saddle periodic orbit under iterations of the RG transformation. Thus, the normalized map describing the evolution of X and Y after a great enough number of time steps (2^{2k} or 2^{2k+1}) will belong to the two-dimensional unstable manifold of the RG cycle:

$$\begin{aligned} \{g(X,Y), f(X,Y)\}_{2k+1} &= \{G_1(X,Y,C_1\delta_1^k, C_2\delta_2^k), F_1(X,Y,C_1\delta_1^k, C_2\delta_2^k)\} \\ \{g(X,Y), f(X,Y)\}_{2k} &= \{G_2(X,Y,C_1\delta_1^k, C_2\delta_2^k), F_2(X,Y,C_1\delta_1^k, C_2\delta_2^k)\} \end{aligned} \tag{19}$$

where

$$G_{1,2}(X,Y,0,0) = g_{1,2}(X,Y) \qquad F_{1,2}(X,Y,0,0)\} = f_{1,2}(X,Y), \tag{20}$$

and $\delta_{1,2}$ are the eigenvalues (18). From (19) we conclude the following about *universality* and *scaling*:

(i) The form of the evolution operator depends only on two coefficients C_1 and C_2;

(ii) The evolution operator is invariant under scale change $C_1 \to C_1/\delta_1$, $C_2 \to C_2/\delta_2$ accompanied by a shift of $k \to k+2$ (the latter means quadrupling of the timescale).

The coefficients $C_{1,2}$ depend on a concrete form of the original map and may be controlled by parameters of this map. It is reasonable to consider C_1, C_2 themselves as convenient parameters for studying unfolding of the C-type criticality. We call C_1 and C_2 *scaling coordinates*.

It follows from our considerations that *formally the codimension of the C-type criticality is two*, i.e. it appears typically in two-parameter families of nonlinear systems. But due to presence of the weakly decaying third eigenmode (see (18)), the distinguishing universal quantitative features of the critical behavior would manifest themselves, in general, only after large enough number of period-doubling bifurcations. However, if an additional third parameter is presented, one may try to tune it to eliminate the weakly decaying mode. For our model (9) this is the case at $b = -0.6663$ or $b = 0.6544$.

3.3. *Infinite self-similar set of attractors at the critical point: Critical quasi-attractor*

Using data from Table 2, one can verify by direct calculations that the map $(X, Y) \to (g_1(X,Y), f_1(X,Y))$ has a stable fixed point with multipliers

$$\mu_1 = -0.725255 \quad \text{and} \quad \mu_2 = 0.847450, \tag{21}$$

and an unstable period-2 cycle with multipliers

$$\mu_1 = -0.848865 \quad \text{and} \quad \mu_2 = 1.174459. \tag{22}$$

Recall that the map (g_1, f_1) is a fixed point of the quadrupling RG transformation: after being successively iterated four times and then rescaled ($X \to X/\alpha_*$, $Y \to Y/\beta_*$) the map returns to itself. Thus, if the point (X^*, Y^*) belongs to a period-4^k cycle of the map (g_1, f_1), then the point $(X^*/\alpha_*, Y^*/\beta_*)$ belongs to the period-4^{k+1} cycle with the same multipliers. Therefore, presence of the stable fixed point implies the existence of stable cycles of periods 4, 16, 64, ... with multipliers equal to the universal values (21). Obviously, each of these coexisting stable

Table 3
Cycles of the map (9) at the C-type critical points

Period	The point (10)		The point (11)	
	x, y	$\mu_{1,2}$	x, y	$\mu_{1,2}$
4	4.70280×10^{-2}	−0.746088	8.77511×10^{-2}	−0.852625
	−0.249667476	0.836959	1.647055174	1.178436
8	-3.29270×10^{-2}	−0.841748	-1.86563×10^{-2}	−0.723036
	−1.303805726	1.171938	1.693668330	0.847867
16	7.10492×10^{-3}	−0.729383	1.33566×10^{-2}	−0.849490
	−1.313341282	0.845411	1.706481364	1.174766
32	-5.04333×10^{-3}	−0.847568	-2.85310×10^{-3}	−0.724878
	−1.315875350	1.174246	1.708642053	0.847642
64	1.07864×10^{-3}	−0.725956	2.03414×10^{-3}	−0.848973
	−1.316306374	0.846812	1.709221776	1.174447
128	-7.68793×10^{-4}	−0.848677	-4.34772×10^{-4}	−0.725202
	−1.316421603	1.174723	1.709320067	0.847534
256	1.64128×10^{-4}	−0.725310	3.09820×10^{-4}	−0.848877
	−1.316441156	0.847087	1.709346278	1.174403
512	-1.17196×10^{-4}	−0.848865	-6.62279×10^{-5}	−0.725256
	−1.316446372	1.174791	1.709350733	0.847509

orbits has its own basin of attraction in the phase space (X, Y). Analogously, the presence of the unstable period-2 cycle means existence of unstable cycles of period 8, 32, 128, ... with multipliers equal to the values (22).

So, the map $(X, Y) \to (g_1(X, Y), f_1(X, Y))$ exhibits an infinite (denumerable) set of coexisting attractors – the cycles of period 4^k, $k = 0, 1, 2, \ldots$. We call this set *a critical quasi-attractor*. Usually a quasi-attractor is regarded as a complex object in phase space containing an infinite number of stable periodic orbits, whereas the empirically observable behavior seems to be chaotic [17]. In our case we talk about the phenomenon that occurs at the border of chaos, admits an RG analysis, and exhibits the properties of quantitative universality and scaling. Note that the map $(X, Y) \to (g_2(X, Y), f_2(X, Y))$ has a critical quasi-attractor that consists of the attractive cycles of periods 2×4^k.

At the critical points of the initial map, the cycles of asymptotically large periods exhibit the same properties. For negative b the multipliers of the period-4^k cycles approach the universal values (21), while those of period-2×4^k tend to the values (22). For positive b the situation is reversed. If the value of b is fitted to optimize the rate of the convergence, the multipliers μ reproduce well the universal values (Table 3).

Fig. 4(a) shows several representatives from the infinite set of attractors for the map (9) at the point (10). The scaling property is illustrated in Fig. 4(b). The patterns reproduce themselves under magnification by factors α_* and β_* along the coordinate axes x and y, respectively.

3.4. *Parameter space topography near the critical point*

As we have mentioned, near the C-type critical point the two-dimensional parameter space will exhibit universal topography in appropriate scaling coordinates (C_1, C_2) (see (19)). Now we want to analyze this universal topography taking the model map (9) as a representative of the universality class.

If we would have explicit expressions for parameters (a, d) via (C_1, C_2) we could reveal the universal self-similar parameter space topography by observing the neighborhood of the critical point under increasing magnification. Applying the scale change $C_1 \to C_1/\delta_1^k$, $C_2 \to C_2/\delta_2^k$ we would see more and more precise coincidence of the pictures for subsequent k. However, because of the asymptotic nature of the universality, it is not necessary to search

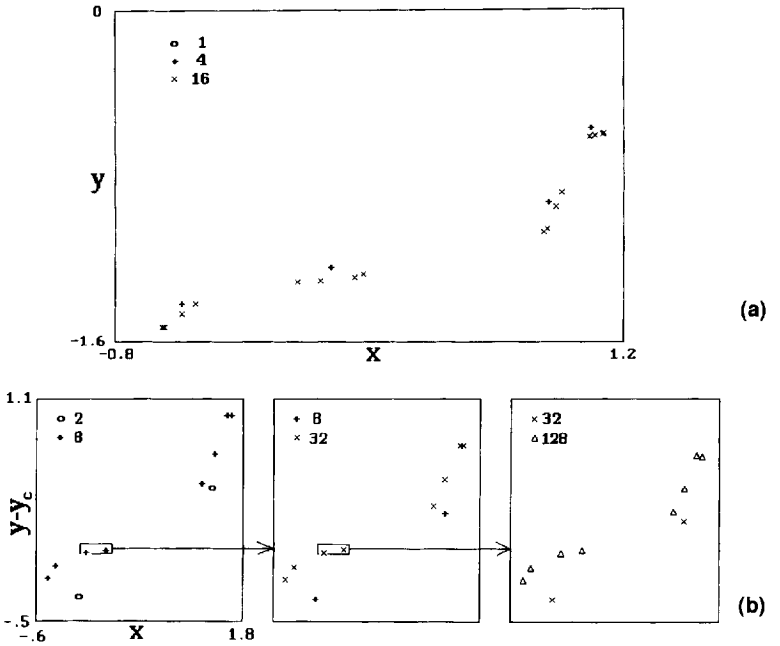

Fig. 4. (a) Representatives of the infinite set of attractors coexisting at the C-type critical point (10) for the map (9). (b) Scaling properties of attractors at the C-type critical point (11). Magnification in each subsequent picture increases by α_* and β_* for horizontal and vertical axes, respectively.

for the exact expressions for the scaling coordinates. It is enough to require the correct results in the asymptotics of small scales (large k).

The condition that a shift from the critical point does not generate the mode with larger eigenvalue δ_1 defines some curve σ in the parameter plane. It is natural to define C_2 as a distance from the critical point along this curve. The other coordinate C_1 may be introduced arbitrarily, the only condition is that the coordinate line must be transversal to the curve σ.

How can we find the curve σ with high enough precision? Suppose, for small ϵ we take $a = a_c + \phi(\epsilon), d = d_c + \varphi(\epsilon)$, were ϕ and φ are some differentiable functions vanishing at the origin. The amplitude of the first mode caused by the perturbation may be represented by Taylor series:

$$C_1 = c_1\epsilon + c_2\epsilon^2 + c_3\epsilon^3 + c_4\epsilon^4 + \cdots \tag{23}$$

To consider subsequent levels of magnification we substitute $C_1 \to C_1/\delta_1^k, \epsilon \to \epsilon/\delta_2^k$ into (23) and obtain

$$C_1 = c_1\epsilon(\delta_1/\delta_2)^k + c_2\epsilon^2(\delta_1/\delta_2^2)^k + c_3\epsilon^3(\delta_1/\delta_2^3)^k + c_4\epsilon^4(\delta_1/\delta_2^4)^k + \cdots \tag{24}$$

For the C-type criticality $\delta_2 < \delta_1, \delta_2^2 < \delta_1, \delta_2^3 < \delta_1$, but $\delta_2^4 > \delta_1$. Thus, we see from (24) that the terms of order 4 and higher vanish in the asymptotic limit of large k. So, there are the first three terms that must be compensated by a proper choice of the functions ϕ and φ.

We accept the following expressions for parameters (a, d) of the model map (9) in terms of new coordinates (C_1, C_2):

$$a = a_c + C_1 - C_2 + qC_2^2 - rC_2^3, \qquad d = d_c - pC_2, \tag{25}$$

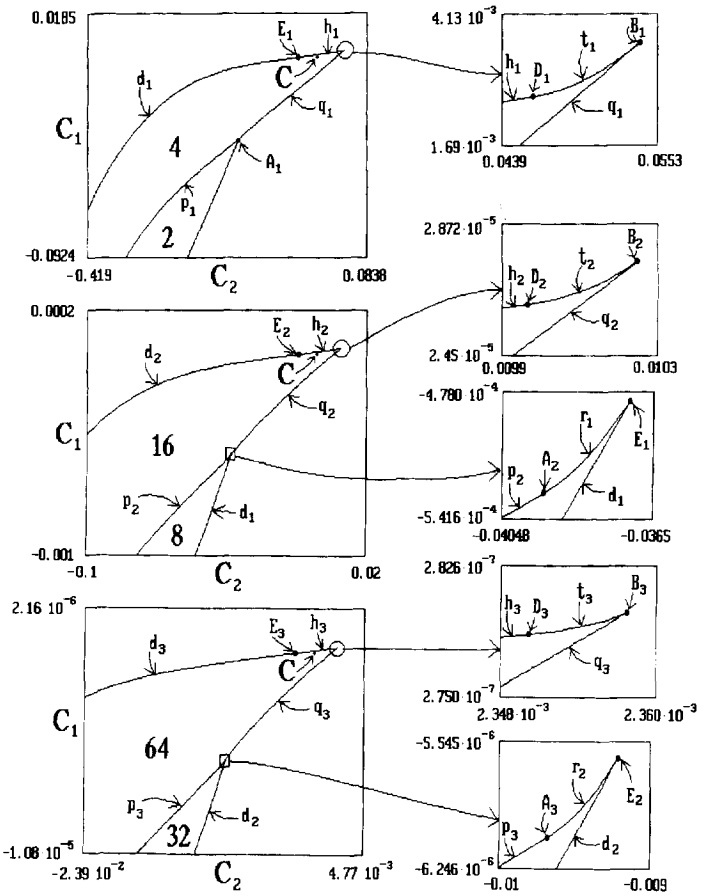

Fig. 5. Stability domains for cycles of periods 2, 4, ..., 64 for the map (9) near the C-type critical point (10). For each subsequent picture the magnification is increased by $\delta_1 = 92.431\ldots$ along the C_1-axis, and by $\delta_2 = 4.192\ldots$ along the C_2-axis. Letters p and d denote the bifurcation curves for birth and stability loss of a cycle via period-doubling, q the Neimark bifurcation, h the "hard" flip bifurcation and t and r denote the saddle–node bifurcations.

where the constants p, q, r are to be found numerically. For this purpose we use multipliers of the orbits of periods 4^k or 2×4^k with large enough k. First, we select p to make the derivatives $\partial\mu_k/\partial C_2$ proportional to δ_2^k. Then, tuning q, we ensure the second derivatives $\partial^2\mu_k/\partial C_2^2$ to behave as δ_2^{2k}, and, finally, select r in such a way that $\partial^3\mu_k/\partial C_2^3 \propto \partial_2^{3k}$. (At each step the number of conditions to be satisfied is larger than the number of unknowns, so it is convenient to use the method of least squares.) We have obtained:

$$\text{for the point (10)}: \quad p = -0.79016607, \quad q = -1.546069, \quad r = 2.15, \tag{26}$$

$$\text{for the point (11)}: \quad p = 0.45431477, \quad q = -0.782222, \quad r = 0.65. \tag{27}$$

In Fig. 5 we use the scaling coordinates in a neighborhood of the critical point (10) to show the stability domains for orbits of periods 4^k and 2×4^k with $k = 1, 2, 3$. Different segments of the stability boundaries are denoted by small letters; capital letters mark the segment junctions. Note that the critical point C belongs to the stability domains of the period-4^k orbits and does not fit into the domains of the period 2×4^k. The pictures are shown under increasing magnification with the factors δ_1 and δ_2 along the vertical and horizontal axes, respectively. Approximate similarity between the pictures gives evidence of the scaling inherent to the vicinity of the critical point C.

The stability boundary of the period-4 orbit contains, first, the segment p_k where this cycle arises via a period-doubling bifurcation (the multipliers are $\mu_1 = 1$ and $|\mu_2| < 1$). This part of the boundary ends at the point $A_k(\mu_1 = \mu_2 = 1)$. From this place, the stability boundary q_k corresponds to Neimark bifurcation giving rise to quasi-periodic dynamics (the multipliers are complex conjugate and $|\mu_1| = |\mu_2| = 1$). The other end of the line q_k is the B_k point (again $\mu_1 = \mu_2 = 1$). The next part of the boundary is a line of "hard" transitions t_k where saddle–node bifurcation occurs ($\mu_1 = 1, |\mu_2| < 1$). The t segment ends at the point $D_k(\mu_1 = 1$ and $\mu_2 = -1)$. The segment h_k corresponds to a "hard" loss of stability when one multiplier traverses the unit circle via -1 (subcritical flip bifurcation). At the point E_k the line h_k turns into usual period-doubling bifurcation line d_k. The stability boundary for the period-2×4^k orbit contains the above mentioned segments, d_k and p_{k+1}. Their end points, A_{k+1} and E_k, are connected by a line r_{k+1} where a saddle–node bifurcation takes place (for the cycle of period 2×4^k one multiplier is equal to 1). At the A_{k+1} point the multipliers are -1 and 1. The terminal point sequence which we use to find the C-type critical point is organized by the points $\ldots D_{k-1}, A_k, D_k, A_{k+1}, D_{k+1}, \ldots$.

Similar behavior is observed in a neighborhood of the second C-type critical point (11); the only difference is that the cycles of periods 4^k and 2×4^k switch their roles.

4. Critical behavior for maps where the singularity arises from the projection of Whitney's umbrella

4.1. Model map and its dynamics

The surface of Whitney's umbrella (Fig. 1(c)) is defined by the relations

$$U = u^2, \quad V = uv, \quad W = v. \tag{28}$$

Projection onto the plane (U, V) yields the two-dimensional map

$$(u, v) \to (u^2, uv), \tag{29}$$

and its composition with a general affine transformation is:

$$(u, v) \to (A + Bu^2 + Cuv, D + Eu^2 + Fuv).$$

Using appropriate variable changes one can reduce the number of parameters to three. Particularly, if $(F - B)^2 + 4EC > 0$, we set

$$x = u/A, \qquad y = (v - \alpha u)(D - \alpha A)^{-1},$$

$$a = -A(B + \alpha C), \quad b = -A(F - \alpha C), \quad d = C(D - \alpha C), \quad \alpha = \frac{F - B + \sqrt{(F - B)^2 + 4EC}}{2C},$$

and obtain

$$x_{n+1} = 1 - ax_n^2 + dx_n y_n, \qquad y_{n+1} = 1 - bx_n y_n. \tag{30}$$

In the above construction we have selected one special projective direction for Whitney's umbrella. If we permit the projective direction to vary, we obtain the modified map with an additional parameter C:

$$x_{n+1} = 1 - ax_n^2 + d(x_n - c)y_n, \qquad y_{n+1} = 1 - b(x_n - c)y_n. \tag{31}$$

Let us arbitrarily fix d=0.3 and consider the topography of the dynamical regimes for the map (30) in the parameter plane (a, b) (Fig. 6). With small b and increasing a the map demonstrates a Feigenbaum period-doubling cascade.

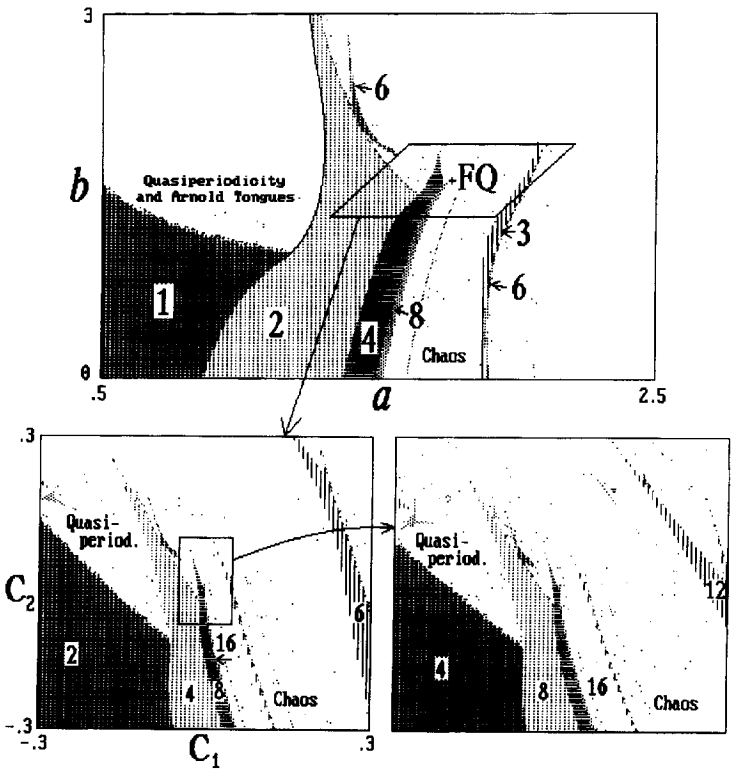

Fig. 6. Topography of the parameter plane (a, b) for the map (30), $d = 0.3$. Stability domains for cycles of different periods are shown with different shading; periods are indicated by numbers. The critical point of FQ-type is marked by a small cross. A neighborhood of this point is shown separately using the scaling coordinate system (40). The second picture at the bottom is shown under magnification along horizontal and vertical axes by $\delta_1 = 6.326\ldots$ and $\delta_2 = 3.444\ldots$, respectively.

Table 4
Terminal points at the period-doubling bifurcation curves for the map (30) ($d = 0.3$)

Period	a	b
1	1.20672845	1.03659636
2	1.65119992	1.50606990
4	1.73958420	1.59072683
8	1.75957972	1.61648798
16	1.76517443	1.62588920
32	1.76665551	1.62862373
64	1.76703430	1.62935673
128	1.76714698	1.62958353
256	1.76718014	1.62965157
∞	1.76719290	1.62967802

For each cycle of period 2^k the stability domain is bounded at larger b by a bifurcation curve corresponding to the onset of quasi-periodicity; this curve terminates at the next line of period-doubling at some bifurcation point. We conjecture that these terminal points form an infinite sequence and converge to a certain limit.

To obtain quantitative data, we start at some small b and find the value of a corresponding to ith period-doubling bifurcation. This implies that one multiplier of the periodic orbit is $\mu_1 = -1$, and μ_2 is in the vicinity of zero. Then we increase b and tune the parameter a to keep $\mu_1 = -1$. Moving in such a way along the bifurcation curve in

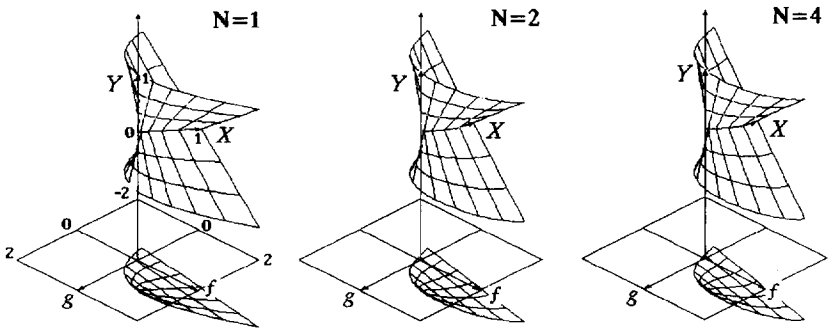

Fig. 7. Geometrical representation of the renormalized two-dimensional maps G_k obtained from N-fold composition of the map (30) at the critical point (32). Observe that the G_k sequence converges to a fixed point of the RG transformation.

Table 5
Critical points FQ in the three-parameter space of the map (30)

d	a	b
0.1	1.5601766	1.8734098
0.2	1.6686977	1.7206404
0.3	1.7671931	0.6296784
0.4	1.8611706	1.5670464
0.5	1.9529898	1.5212836
0.6	2.0439580	1.4869291
0.7	2.1348970	1.4608887
0.8	2.2263624	1.4412048
0.9	2.3187446	1.4265424
1.0	2.4123208	1.4159365

the parameter plane (a, b), we arrive at the terminal point (a_i, b_i) where $\mu_1 = \mu_2 = -1$. Parameter values for the terminal points at several period-doubling lines are presented in Table 4. Estimating the limit of the terminal point sequence we have found

$$\text{for } d = 0.3: \qquad a_c = 1.767192895, \quad b_c = 1.629678013. \tag{32}$$

We denote this point as "FQ", since the period-doubling (symbol "F", Feigenbaum) and quasi-periodicity (symbol "Q") occur in any small vicinity of this point. Critical points of the same nature may be found for other values of d, both negative and positive. In the three-parameter space (a, b, d) there exists a curve which is the locus of these FQ points (Table 5).

4.2. *Renormalization group fixed point and its perturbations*

The critical behavior at the FQ point is associated with a saddle fixed point of the RG equation (4). It may be demonstrated numerically by carrying out multiple iterations of the RG transformation of the model map (30). First, we must choose an appropriate coordinate system in phase space – scaling variables X and Y. Having found the period-2^k orbits at the parameter values (32) we observe that for large k the points of the orbits fall near the origin on the line $y = \rho x$, $\rho = 2.1091$. Thus, we introduce new variables X and Y by relations $x = X$, $y = Y + \rho X$ and rewrite the map (30) as

Table 6
Polynomial approximations for the universal functions g, f, corresponding to the FQ fixed point of the RG equation (4)

	1	Y	Y^2	Y^3	Y^4	Y^5
$g(x, y)$						
1	1.000000	0.000000	−0.000003	0.000000	0.000002	
X	0.000000	−0.711423	0.000000	0.000005	0.000000	
X^2	−1.097926	0.000000	0.001860	0.000000	−0.000025	
X^3	0.000000	0.086519	0.000000	0.007119	0.000000	
X^4	0.157331	0.000000	0.037350	0.000000	−0.000294	
X^5	0.000000	0.043877	0.000000	−0.003629	0.000000	
X^6	−0.018284	0.000000	−0.013299	0.000000		
X^7	0.000000	−0.017820	0.000000	0.000519		
X^8	−0.005775	0.000000	0.002289	0.000000		
X^9	0.000000	0.003437	0.000000			
X^{10}	0.001913	0.000000				
$f(x, y)$						
1	1.000000	0.000000	−0.000003	0.000000	0.000003	0.000000
X	0.000000	−2.796050	0.000000	0.000233	0.000000	−0.000085
X^2	0.066947	0.000000	0.210253	0.000000	−0.000092	0.000000
X^3	0.000000	1.362135	0.000000	−0.005578	0.000000	0.000688
X^4	1.541702	0.000000	−0.158674	0.000000	−0.003899	0.000000
X^5	0.000000	−0.816413	0.000000	−0.016455	0.000000	−0.000362
X^6	−1.061435	0.000000	−0.007651	0.000000	0.009521	0.000000
X^7	0.000000	0.179277	0.000000	0.033055	0.000000	0.000000
X^8	0.197242	0.000000	0.065557	0.000000	−0.004133	0.000000
X^9	0.000000	−0.003142	0.000000	−0.010749	0.000000	
X^{10}	−0.012557	0.000000	−0.018792	0.000000		

$$G_0: \quad X_{n+1} = g_0(X_n, Y_n), \quad Y_{n+1} = f_0(X_n, Y_n),$$

where

$$g_0(X_n, Y_n) = 1 + (-a_c + \rho d)x_n^2 + dX_nY_n,$$
$$f_0(X_n, Y_n) = 1 + \rho(-b_c + a_c - \rho d)X_n^2 - (b_c - \rho d)X_nY_n. \tag{33}$$

Taking the map G_0 as initial condition for the iterations of the RG transformation (4) we can calculate numerically the maps G_k by relations similar to (14). In Fig. 7 the plots of these maps are presented for several values of k. It is reasonable to conjecture their convergence to a certain limit. This will be a fixed point of the RG equation (4): $\lim G_k = G_{FQ} = \{g, f\}$, where g and f must satisfy the equations

$$g(X, Y) = \alpha g(g(X/\alpha, Y/\beta), f(X/\alpha, Y/\beta)),$$
$$f(X, Y) = \beta f(g(X/\alpha, Y/\beta), f(X/\alpha, Y/\beta)), \tag{34}$$

$$\alpha = 1/g(1, 1), \quad \beta = 1/f(1, 1). \tag{35}$$

To obtain the solution numerically we approximate the functions g and f by polynomials with unknown coefficients and reduce the problem (34) to a finite set of nonlinear algebraic equations. Then, it is solved by the Newton–Raphson technique taking one of the maps G_k as the first approximation. In Table 6 we present the coefficients of the polynomial expansions for the functions g and f. The scaling factors are

$$\alpha = -1.90007167 \quad \text{and} \quad \beta = -4.00815785. \tag{36}$$

Table 7
Cycles of the map (30) at the FQ-type critical point (32)

Period	x	y	μ_1	μ_2
1	0.550850	0.526951	−1.581202	−1.105341
2	−0.244687	−0.309739	−1.619623	−1.031132
4	0.124889	0.206623	−1.591129	−1.037311
8	−0.066536	−0.126188	−1.572453	−1.072403
16	0.034915	0.070079	−1.584673	−1.057193
32	−0.018212	−0.037495	−1.585264	−1.045115
64	0.009648	0.020120	−1.573862	−1.063807
128	−0.005091	−0.010681	−1.579422	−1.062196
256	0.002662	0.005601	−1.584243	−1.049598
512	−0.001404	−0.002957	−1.577460	−1.057984
1024	0.000741	0.001563	−1.577896	−1.062400

The next step of the RG analysis consists in the consideration of small perturbations to the fixed point of the RG transformation. Linearization of Eqs. (4) leads to the following eigenproblem:

$$\begin{aligned}\delta u(X,Y) &= \alpha[g_1'(g(X/\alpha, Y/\beta), f(X/\alpha, Y/\beta))u(X/\alpha, Y/\beta)\\ &\quad + g_2'(g(X/\alpha, Y/\beta), f(X/\alpha, Y/\beta))v(X/\alpha, Y/\beta) + u(g(X/\alpha, Y/\beta), f(X/\alpha, Y/\beta))],\\ \delta v(X,Y) &= \beta[f_1'(g(X/\alpha, Y/\beta), f(X/\alpha, Y/\beta))u(X/\alpha, Y/\beta)\\ &\quad + f_2'(g(X/\alpha, Y/\beta), f(X/\alpha, Y/\beta))v(X/\alpha, Y/\beta) + v(g(X/\alpha, Y/\beta), f(X/\alpha, Y/\beta))],\end{aligned} \tag{37}$$

where subscripts 1 and 2 mark the derivatives with respect to the first and the second argument of the functions. Computer solution of this problem shows that there exist three relevant eigenvectors; the corresponding eigenvalues are: [1]

$$\delta_1 = 6.32631925, \qquad \delta_2 = 3.44470967, \qquad \delta_3 = \alpha = -1.90007167. \tag{38}$$

Hence, *the total codimension of the FQ-type criticality is three*. In general, one should expect to observe this criticality typically in a three-parameter analysis. In the model map (30) we have found the point FQ by fitting only two parameters because of using the special projective direction for Whitney's umbrella. In the more general model map (31) the FQ-type criticality actually appears as a codimension-three phenomenon. Accordingly, only two eigenvalues δ_1 and δ_2 are responsible for the parameter space scaling properties of the map (30), and all three eigenvalues (38) are relevant for the map (31).

4.3. Dynamics at the critical point and fractal structure of the critical attractor

Using the data of Table 6, one can check by direct calculations that the map $(X, Y) \to (g(X, Y), f(X, Y))$ has an unstable fixed point with multipliers

$$\mu_1 = -1.579739 \quad \text{and} \quad \mu_2 = -1.057149. \tag{39}$$

We know that according to the RG equation the map (g, f) iterated twice and rescaled $(X \to X/\alpha, Y \to Y/\beta)$ returns to itself. Hence, the presence of the fixed point implies existence of unstable cycles of period 2, 4, 8, ...

[1] In fact, the eigenvalue α in the spectrum of the linearized RG equation operator appears to be doubly degenerate. However, only one of the corresponding two components of perturbations is relevant. The other is associated with an infinitesimal variable change $X \to X + \epsilon$ and always can be eliminated by a shift of the origin for the dynamical variable.

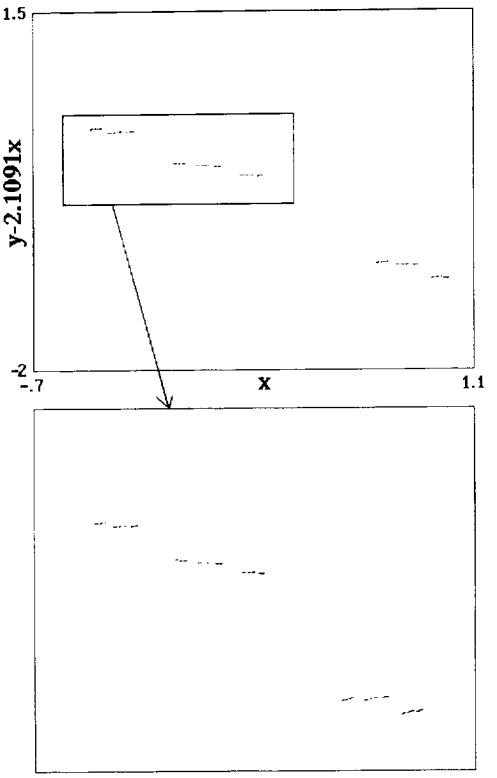

Fig. 8. Self-similar structure of the attractor for the map (30) at the FQ critical point (32). Rescaling is produced along horizontal and vertical axes by $\alpha = -1.900\ldots$ and $\beta = -4.008\ldots$, respectively.

possessing the same multipliers. If (X^*, Y^*) is the fixed point then the point $(X^*/\alpha^k, Y^*/\beta^k)$ belongs to the period-2^{k+1} orbit. We conclude that the map $(X, Y) \to (g(X, Y), f(X, Y))$ exhibits an infinite (denumerable) set of unstable cycles of period 2^k.

In the asymptotic limit of large periods the same properties will be valid for any map exhibiting the FQ-type criticality. In Table 7 the multipliers are presented for periodic orbits of the map (30) at the point (32). Observe that they accurately reproduce the universal values (39).

The attractor at the critical point FQ is a limit object, "period-2^∞ cycle". It is a fractal set embedded in two-dimensional phase space. In Fig. 8 the attractor is shown in the scaling coordinate system (X, Y), and its properties of self-similarity are illustrated: a part of the configuration (outlined by a small box) reproduces the overall pattern under the magnification by the factors of α and β along the coordinate axes. A procedure of constructing the fractal attractor is presented in Fig. 9. Let us consider a sequence X_n, Y_n generated by iterations of the map (33) starting from $X_0 = 0$, $Y_0 = 0$. At this initial point there are two scaling eigendirections, defined by vectors $\boldsymbol{i}_0 = \{1, 0\}$ and $\boldsymbol{j}_0 = \{0, 1\}$. Also, each point X_n, Y_n may be characterized by a pair of vectors $\boldsymbol{i}_n, \boldsymbol{j}_n$ – the directions of the n-fold iterated initial small perturbations of X and Y. (For example, $\boldsymbol{i}_1 = \{-a_c + \rho d_c, \rho(-b + a_c - \rho d_c)\}, \boldsymbol{j}_1 = \{d_c, -b + \rho d_c\}$.) At first, we take the points with $n = 1$ and 2 and draw straight lines along the corresponding vectors $\boldsymbol{i}$ and $\boldsymbol{j}$ to form a quadrangle (Fig. 9(a)).

Second, we take the points with $n = 1$ and 3, 2 and 4, and in a similar way build two quadrangles inside the previous one. At the kth step of the procedure we take 2^k pairs of the points $X_{n+2^{k-1}}, Y_{n+2^{k-1}}, n = 1, \ldots 2^k$, and

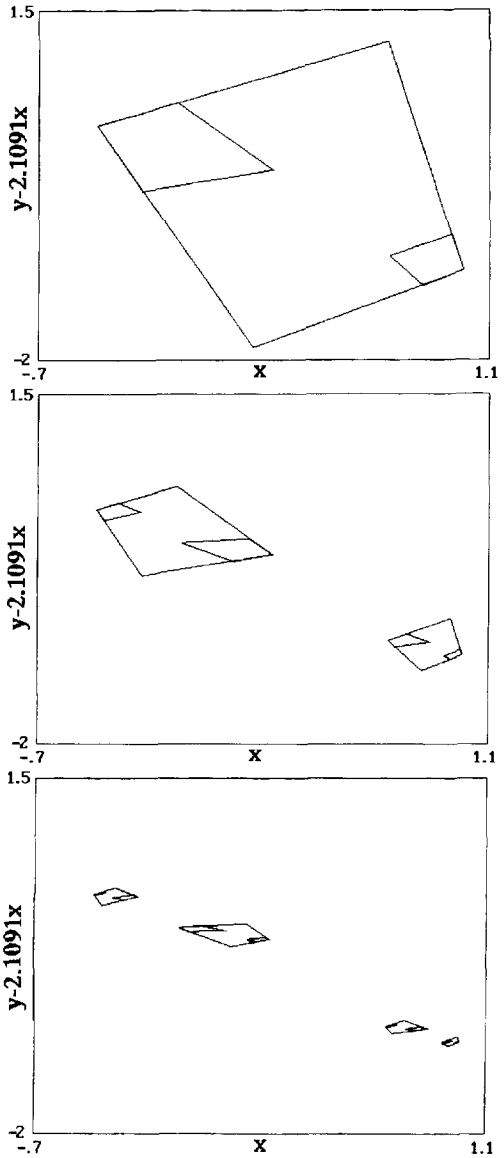

Fig. 9. Construction of the critical attractor at the point FQ in analogy with Cantor set: at each step the points are eliminated that are outside the next generation of quadrangles.

build 2^k quadrangles with sides along the vectors $\boldsymbol{i}_{n+2^{k-1}}, \boldsymbol{j}_{n+2^{k-1}}$. Unification of these 2^k quadrangles is the kth level of approximation for the fractal attractor (Figs. 9(b) and (c)).

4.4. *Parameter space topography and its scaling properties*

Let us return to the topography of the dynamical regimes for the map (30) in the parameter plane (a, b) (Fig. 6). One can see that near the point FQ the details of the pattern repeat themselves on smaller and smaller scales. To demonstrate quantitative self-similarity of the period-doubling it is necessary to find the scaling coordinate system

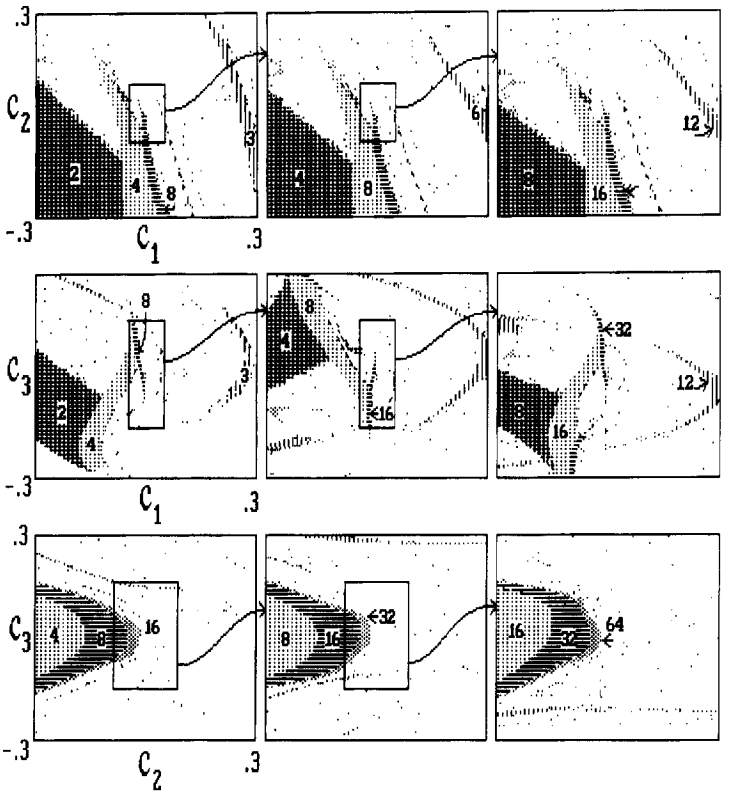

Fig. 10. Scaling properties of the three-dimensional parameter space of the map (31) in the neighborhood of the FQ critical point ($a = 1.767192\ldots, b = 1.629678\ldots, c = 0, d = 0.3$). The pictures correspond to cross-sections of the parameter space (a, b, c) by coordinate surfaces (C_i, C_j) (see (41)). The critical point is located exactly at the center of each picture. Domains of existence for attractive cycles with different periods are shown by different shading. Magnification factors along horizontal and vertical axes for each sequence of the pictures are the numbers δ_i, δ_j given by (38).

(C_1, C_2). (A parameter shift from the critical point along a new coordinate axis C_i must generate a perturbation with a definite eigenvalue of the linearized RG equation.)

For the present case, only δ_1 and δ_2 are relevant. Note that $\delta_2^2 \geq \delta_1$. Thus, considerations analogous to those in Section 3.4 show that (a, b) may be expressed via (C_1, C_2) simply by an affine transformation. We place the origin at the critical point (32) and arbitrarily define the coordinate C_1 along the a-axis. For the second coordinate C_2 we take a linear combination of $\Delta a = a - a_c$ and $\Delta b = b - b_c$ with a coefficient fitted numerically to make the derivatives $\partial \mu_k / \partial C_2$ for large k to be proportional to δ_2^k. In such a way, we have found

$$a = a_c + C_1 + pC_2, \quad b = b_c + C_2, \qquad p = 0.4773293. \tag{40}$$

The area inside the parallelogram in the parameter plane of Fig. 9 is shown separately in scaling coordinates. Observe that the picture reproduces itself well under rescaling by the factors δ_1 and δ_2 along the respective coordinate axes. The smaller the neighborhood of the critical point is, the better the correspondence will be.

Let us turn now to a modified map (31) for the same $d = 0.3$ and consider the scaling properties of the three-dimensional parameter space (a, b, c) near the critical point of FQ-type $(a_c, b_c, 0)$. In this case, all three eigenvalues $\delta_1, \delta_2, \delta_3$ are relevant. Note that $\delta_3^2 < \delta_1$, but $|\delta_2 \delta_3| > \delta_1$ and $|\delta_3^3| > \delta_1$. Analysis similar to that in Section 3.4 shows that we must account for the term C_3^2 but not for other additional nonlinear terms in the relations for (a, b)

via (C_1, C_2). So, we write

$$a = a_c + C_1 + pC_2 + qC_3 + sC_3^2, \qquad b = b_c + C_1 + rC_2, \qquad c = C_3, \tag{41}$$

and numerically obtain the following coefficients:

$$p = 0.4773293, \quad q = -0.2299895, \quad r = 0.4649090, \quad s = -2.9.$$

Fig. 10 depicts the topography of the dynamical behavior near the critical point FQ for three cross-sections of the parameter space (a, b, c) by coordinate surfaces (C_i, C_j). The critical point is located exactly at the center of each picture. Domains of cycles of different periods are shown with different shadings. The outlined rectangles are reproduced with vertical and horizontal magnification by the corresponding factors δ_i, δ_j. Observe that location and shape of the domains of different dynamical regimes repeat themselves on smaller scales.

5. Conclusions

When studying dynamical systems in terms of differential equations with the help of the Poincaré section technique, the maps obtained will be inevitably *invertible*. Nevertheless, it is reasonable to use one-dimensional *non-invertible* maps to describe *approximately* dynamics of dissipative systems with phase space dimension ≥ 3. Moreover, owing to Feigenbaum, we know that the behavior of a great number of nonlinear systems at the onset of chaos via period-doubling is related to the same universality class as one-dimensional non-invertible maps with a quadratic extremum.

Analogously, non-invertible two-dimensional maps may be useful to describe the dynamics of nonlinear dissipative systems with phase space dimension ≥ 4. We believe that for such systems the C- and FQ-types of critical dynamics may be met as generic phenomena during a multi-parameter analysis of transition to chaos. The maps (9) and (31) are the representatives of the universality classes for the new types of critical behavior and play the same role as the logistic map plays for the classic Feigenbaum period-doubling.

It seems possible to observe critical behavior of C-type in a following situation. Suppose we have a dynamical system which is controlled by two parameters; increasing one parameter implies period-doubling cascade, and tuning the second one gives rise to a tangent or saddle–node bifurcation ("intermittency"). Such a case often occurs in a two-parameter analysis of the transition to chaos, for example, in periodically driven chaotic systems. In the bifurcation diagrams for electronic systems presented in books [17, pp. 149, 152] and [18, p. 131] one can see clearly that the lines of period-doubling inside Arnold's tongues stick into their edges. It seems likely that the critical points of C-type exist in these regions of parameters.

Another possibility to realize both C- and FQ-types of criticality consists in consideration of coupled systems. In accordance with [19–21], the dynamics of two periodically driven coupled LCR-circuits with semiconductor diodes can be described well by a system of two coupled logistic maps. Such coupled map system was the first model for which we have found numerically the types of critical behavior discussed here [11]. In [21] some details characteristic for the neighborhood of the C-type critical point may be seen in the experimentally obtained bifurcation diagram.

We believe that in spite of obvious difficulties, observation and identification of the new types of critical behavior are possible. However, the experimental setup must be specially designed to account for the information presented here on the nature and properties of the critical dynamics.

Acknowledgements

We are grateful to Prof. Raymond Kapral and to Prof. Erik Mosekilde for useful discussion and comments. This work is supported by the grant number 95-02-05818 of Russian Fund of Fundamental Research.

References

[1] M.J. Feigenbaum, J. Statist. Phys. 19 (1978) 25.
[2] M.J. Feigenbaum, J. Statist. Phys. 21 (1979) 669.
[3] O.E. Lanford, Bull. Amer. Math. Soc. (1982) 427.
[4] B. Hu and I. Satija, Phys. Lett. A 98 (1983) 143.
[5] S.J. Chang, M. Wortis and J. Wright, Phys. Rev. A 24 (1981) 2669; S. Fraser and R. Kapral, Phys. Rev. A 25 (1984) 3223.
[6] A.P. Kuznetsov, S.P. Kuznetsov and I.R. Sataev, Phys. Lett. A 189 (1994) 367.
[7] C. Mira, Chaotic Dynamics (World Scientific, Singapore, 1987).
[8] H. Whitney, Ann. Math. 62 (1955) 374.
[9] V.I. Arnold, A.N. Varchenko and S.M. Gusein-Zade, Singularities of Differentiable Mappings (Osobennosti differentsiruemykh otobrazhenii, Nauka, Moscow, 1982).
[10] V.I. Arnold, Catastrophe Theory (Teoriya katastrof, Nauka, Moscow, 1990).
[11] S.P. Kuznetsov and I.R. Sataev, Phys. Lett. A 162 (1992) 236.
[12] R.S. MacKay and J.B.J. van Zeijts, Nonlinearity 1 (1988) 253.
[13] J.P. Eckmann, H. Koch and P. Wittwer, Phys. Rev. A 26 (1982) 720; M. Widom and L. Kadanoff, Physica D 5 (1982) 287.
[14] G. Schmidt, in: Directions in Chaos, ed. Hao Bai-lin, Vol. 2 (1988) 1.
[15] A.P. Kuznetsov, S.P. Kuznetsov and I.R. Sataev, Int. J. Bifurc. and Chaos 1 (1992) 839.
[16] A.P. Kuznetsov, S.P. Kuznetsov and I.R. Sataev, Int. J. Bifurc. and Chaos 3 (1993) 139.
[17] V.S. Anishchenko, Dynamical Chaos–Models and Experiments. Appearance, Routes and Structure of Chaos in Simple Dynamical Systems (World Scientific, Singapore, 1995).
[18] A.S. Dmitriev and V.Ya. Kislov, Stochastic Oscillations in Radio-Physics and Electronics (Stokhasticheskie kolebaniya v radiofizike i elektronike, Nauka, Moscow, 1989).
[19] B.P. Bezruchko, Yu.V. Gulyaev, S.P. Kuznetsov and E.P. Seleznev, Soviet Phys. Dokl. 31 (1986) 258.
[20] V.V. Astakhov, B.P. Bezruchko, Y.N. Yerastova and E.P. Seleznev, Zhurnal Tekhn. Fiz. 60 (10) (1990) 19.
[21] V.V. Astakhov, B.P. Bezruchko, S.P. Kuznetsov and E.P. Seleznev, Soviet Tech. Phys. Lett. 14 (1988) 16.
[22] T.S. Halsey, M.H. Jensen, L.P. Kadanoff, I. Procaccia and B.I. Shraiman, Phys. Rev. A 33 (1986) 1141.
[23] P. Berge, Y. Pomeau and C. Vidal, Order within Chaos, Towards a Deterministic Approach to Turbulence (Wiley, New York, 1986).